Inorganic Chemistry

ARTICLE

pubs.acs.org/IC

Validation of Speciation Techniques: A Study of Chlorozincate(II) Ionic Liquids

Julien Estager, Peter Nockemann, Kenneth R. Seddon,* Małgorzata Swadźba-Kwaśny, and Sophie Tyrrell

QUILL, The Queen's University of Belfast, Belfast BT9 5AG, United Kingdom

Supporting Information

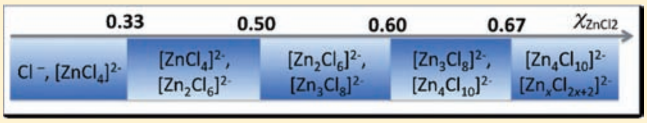

ABSTRACT: The speciation of chlorozincate(II) ionic liquids, prepared by mixing 1-octyl-3-methylimidazolium chloride, $[C_8mim]Cl$, and zinc(II) chloride in various molar ratios, χ_{ZnCl_2}, was investigated using Raman spectroscopy and differential scanning calorimetry; the Gutmann acceptor number, which is a quantitative measure of Lewis acidity, was also determined as a function of the composition. These results were combined with literature data to define the anionic speciation; in the neat liquid phase, the existence of Cl^-, $[ZnCl_4]^{2-}$, $[Zn_2Cl_6]^{2-}$, $[Zn_3Cl_8]^{2-}$, and $[Zn_4Cl_{10}]^{2-}$ anions was confirmed. From two chlorozincate(II) ionic liquids with $[C_2mim]^+$ cations (χ_{ZnCl_2} = 0.33 and χ_{ZnCl_2} = 0.50), crystals have been obtained, revealing the structures of $[C_2mim]_2[ZnCl_4]$ and $[C_2mim]_2[Zn_2Cl_6]$ forming three-dimensional hydrogen-bond networks. The compound $[C_2mim]_2\{Zn_4Cl_{10}\}$ was crystallized from the χ_{ZnCl_2} = 0.75 composition, showing an open-framework structure, with the first example of zinc in a trigonal-bipyramidal chloride coordination. Reinvestigation of the electrospray ionization mass spectrometry of these systems demonstrated that it is an unreliable technique to study liquid-phase speciation.

INTRODUCTION

Ionic liquids are compounds composed exclusively of ions: usually a bulky organic cation and an organic or inorganic anion.[1] By the direct mixing of a metal chloride with an organic chloride salt (e.g., 1-alkyl-3-methylimidazolium chloride, $[C_nmim]Cl$, $n = 1-18$), it is possible to synthesize chlorometallate ionic liquids with very interesting and potentially useful properties. It is well established that their reactivity, e.g., their Lewis acidity or basicity, depends on both the nature of the metal incorporated in an ionic liquid and the ratio of metal chloride to organic chloride salt used for its synthesis (expressed commonly as the effective mole fraction of "monomeric" metal chloride, χ_{MClx}).[2] Through tuning of these two factors, it is possible to modify the anionic speciation of an ionic liquid and, consequently, control its catalytic acitvity (for example, Lewis acidity is related to the presence of anionic polynuclear species, $[M_xCl_y]^{z-}$, in a given composition of a chlorometallate ionic liquid).[2,3]

Chlorometallate systems based on aluminum have been investigated because of their novel electrochemical properties, with a focus on electrodeposition and battery applications.[4] Although they were extensively examined[4,5] and applied industrially,[6] their extreme instability toward moisture posed a major barrier to their general applicability. Subsequently, other group 13 metal(III) chlorides, indium(III) chloride[7−9] or gallium(III) chloride[10−12] have been used to synthesize ionic liquids, and their anionic speciation has been thoroughly studied, as summarized in Table 1. Remarkably, each of these group 13 metals has a unique anionic speciation and reactive chemistry, despite assumptions of commonality in the literature. In addition, chloroferrate(III) systems[13] have also been examined, but to a lesser extent; Raman spectroscopic studies confirm the existence of $[FeCl_4]^-$ in all compositions and, for $\chi_{FeCl_3} > 0.50$, $[Fe_2Cl_7]^-$ was also detected.[13]

In switching from oxidation state 3+ to 2+, the chlorometallate(II) ionic liquids are found to have generally higher melting points and to be much more viscous.[14] Although many chlorometallate(II) salt systems have been reported in the literature,[15] these traditionally have been considered as salts containing inorganic anions, and their behavior, in the molten state, as ionic liquids has rarely been considered. However, a number of applications as ionic liquids have been described, e.g., chlorocuprate(II) systems as catalysts for aerobic oxidation[16] and as precursors for the synthesis of copper(I) chloride nanostructures[17] and chlorozincate(II) ionic liquids for electrodeposition of zinc or zinc-containing alloys[18] and as reaction media and Lewis acidic catalysts for a range of processes, including the Fischer indole reaction,[19] O-acetylation of cellulose,[20] or protection of aldehydes.[21] Furthermore, a number of chlorometallate(II) ionic liquid crystals have been studied.[22]

The speciation of such chlorometallate(II) systems has not been thoroughly examined or well-established. It has been reported, for example, that chloroferrate(II) ionic liquids contain $[FeCl_4]^{2-}$ and form homogeneous liquids for $\chi_{FeCl_2} \leq 0.50$ compositions,[13] whereas chlorocuprate(II) systems seem to incorporate mainly $[CuCl_4]^{2-}$, in equilibrium with $[Cu_2Cl_6]^{2-}$ for higher χ_{CuCl_2} values (solution studies).[23]

In a continuation of our studies on Lewis acidic ionic liquids,[2,11,8] the most Lewis acidic metal of the first-row transition metals, zinc, was examined; the cynosure is the speciation of chlorozincate(II) anions, and its conclusions are surprisingly far-ranging.

Received: March 24, 2011
Published: May 05, 2011

Table 1. Major Anions Present in Chlorogallate(III), Chloroindate(III), and Chloroaluminate(III) Systems as a Function of the Composition, χ_{MCl_3}[5,8,11]

χ_{MCl_3}					
0.25	0.33	0.50	0.67	0.75	>0.75
$[InCl_6]^{3-}$	$[InCl_5]^{2-}$	$[InCl_4]^-$		$[InCl_4]^-$, $InCl_3\downarrow$	
Cl^-, $[GaCl_4]^-$		$[GaCl_4]^-$	$[GaCl_4]^-$, $[Ga_2Cl_7]^-$	$[Ga_2Cl_7]^-$, $[Ga_3Cl_{10}]^-$	$[Ga_3Cl_{10}]^-$, $[Ga_4Cl_{13}]^-$
Cl^-, $[AlCl_4]^-$		$[AlCl_4]^-$	$[AlCl_4]^-$, $[Al_2Cl_7]^-$	$[Al_2Cl_7]^-$, $[Al_3Cl_{10}]^-$, $[Al_2Cl_6]\downarrow$	$[Al_3Cl_{10}]^-$, $[Al_4Cl_{13}]^-$, $[Al_2Cl_6]\downarrow$

Table 2. Weight (m) of the Reactants (g) for the Synthesis of $[C_n\text{mim}]Cl-ZnCl_2$ (n = 2 or 8) Systems

	n = 2			n = 8	
χ_{ZnCl_2}	$m_{[C_2mim]Cl}$	m_{ZnCl_2}	χ_{ZnCl_2}	$m_{[C_8mim]Cl}$	m_{ZnCl_2}
0.2503	1.9096	0.5928	0.1006	3.7683	0.2490
0.3307	1.7152	0.7878	0.2001	3.4725	0.5131
0.5000	1.2955	1.2045	0.3010	3.2044	0.8148
0.6001	1.0444	1.4572	0.3300	7.0655	2.0553
0.6700	0.8660	1.6346	0.4000	5.7290	2.2554
0.7500	0.6601	1.8412	0.4599	5.3568	2.6942
0.8001	1.0605	3.9450	0.4850	5.1857	2.8840
			0.5003	4.6739	2.7639
			0.5500	4.6410	3.3502
			0.6000	3.6117	3.1994
			0.6702	3.2072	3.8495
			0.7000	3.3841	4.6635
			0.7500	2.7474	4.8681
			0.8502	1.1507	3.8562

Zinc(II) chloride is known to react with a range of organic chloride salts, such as quaternary ammonium chloride,[24] 1-alkyl-3-methylimidazolium chloride,[25] or 1-alkylpyridinium chloride,[26] to form ionic liquids.[27] A number of reported applications of those systems[18−21] have inspired speciation studies,[28−33] which have proven to be inconclusive.

In this work, we critically analyze extant literature data and present novel structural, spectroscopic, and Lewis acidity studies of $[C_n\text{mim}]Cl-ZnCl_2$ (n = 2 or 8) systems, which allow a definitive statement to be made about the speciation.

EXPERIMENTAL SECTION

Zinc(II) chloride (99.99%; anhydrous beads packed under argon in glass ampules) and triethylphosphine oxide (tepo) were purchased from Sigma-Aldrich and opened in a dinitrogen-filled glovebox (Mbraun LabMaster dp; <0.1 ppm O_2 and H_2O). 1-Ethyl-3-methylimidazolium chloride was purchased from Merck, recrystallized from a mixture of ethanenitrile and ethyl ethanoate, and dried under high vacuum (7 days, 70 °C) before placing it in the glovebox. 1-Octyl-3-methylimidazolium chloride was prepared as described elsewhere.[8] All compounds were stored in the glovebox.

Synthesis of $[C_n\text{mim}]Cl-ZnCl_2$ (n = 2 or 8) Systems. A range of compositions ($0.25 \leq \chi_{ZnCl_2} \leq 0.85$) of chlorozincate(II) ionic liquids based on 1-octyl-3-methylimidazolium or 1-ethyl-3-methylimidazolium cations were prepared on a 2−8 g scale. Homogenous liquids were formed for $0.25 \leq \chi_{ZnCl_2} \leq 0.75$ samples. In the glovebox, an appropriate amount of $[C_n\text{mim}]Cl$ (Table 2) was weighed into a sample vial (10 cm^3) equipped with a stirring bar.

Leaving the vial on the balance (±0.0002 g), an appropriate amount of zinc(II) chloride was added very carefully to achieve the desired composition. Subsequently, the sample vial was closed with a cap, placed directly in a multiwell heater−stirrer (80−130 °C, depending on the composition), and stirred vigorously overnight. Samples were stored in the glovebox prior to the study.

ANALYTICAL METHODS

Mass Spectrometry. Electrospray ionization mass spectroscopy (ESI-MS) experiments were carried out using a Waters LCT Premier instrument with an AdvionTriVersaNanoMate injection system (cone voltage 50 V; source 120 °C). Both positive and negative ions were detected, with a range of m/z 50−1500. Samples were injected as dilute solutions in ethanenitrile.

Raman Spectroscopy. Raman spectra were recorded using a Perkin-Elmer RamanStation 400F spectrometer, with a 785 nm focused laser beam. The neat samples were loaded in the glovebox to standard 10 mm quartz cuvettes, closed with a Teflon cap, and sealed with parafilm. They were removed from the glovebox immediately prior to the measurement. Five 5 s scans were recorded for each sample.

Crystallography. Crystal data for $[C_2mim]_2[ZnCl_4]$, $[C_2mim]_2[Zn_2Cl_6]$, and $[C_2mim]_2\{Zn_4Cl_{10}\}$ were collected using a Bruker Nonius Kappa CCD diffractometer with a FR591 rotating anode and a molybdenum target at ca. 120 K in a dinitrogen stream. Lorentz and polarization corrections were applied. The structures were solved by direct methods. Hydrogen-atom positions were located from difference Fourier maps, and a riding model with fixed thermal parameters ($U_{ij} = 1.2U_{eq}$ for the atom to which they are bonded; 1.5 for methyl) was used for subsequent refinements. The function minimized was $\Sigma[\omega(|F_o|^2 - |F_c|^2)]$ with reflection weights $\omega^1 = [\sigma^2\,|F_o|^2 + (g_1P)^2 + (g_2P)]$, where $P = [\max|F_o|^2 + 2|F_c|^2]/3$. The *SHELXTL* package and OLEX2 were used for structure solution and refinement.[34,35]

Differential Scanning Calorimetry (DSC). All scans were obtained using a TA DSC Q2000 model with a TA 90 refrigerated cooling system and an autosampler. The samples were sealed in the glovebox in TA Tzero alodined pans with hermetic alodined lids. The temperature was ramped from +25 to −90 °C, at 10 °C min^{-1}, then stabilized at −90 °C for 10 min, subsequently heated to 40 °C, at 1 °C min^{-1}, and then stabilized at 40 °C for 5 min, and the whole cycle was repeated. The DSC chamber was filled with a dry dinitrogen gas.

^{31}P NMR Spectroscopy Experiments for Gutmann Acceptor Number (AN) Calculations. Sample preparation was carried out in the glovebox. A sample (ca. 1 g) of each composition was weighed into a sample vial (10 cm^3) equipped with a poly(tetrafluoroethylene)-coated magnetic stirring bar. The vial was

Table 3. Quantities of Components for the [C_8mim]Cl−$ZnCl_2$ System Used To Prepare Solutions for ^{31}P NMR Spectroscopy

		m/g	
χ_{ZnCl_2}	tepo/mol %	[C_8mim]Cl−$ZnCl_2$	tepo
0.0000	5.0710	1.0041	0.0296
	10.0330	1.0030	0.0585
	14.9820	1.0012	0.0872
0.1006	5.1678	1.0007	0.0282
	10.5200	1.0006	0.0574
	15.2362	1.0002	0.0831
0.2001	4.9754	1.0000	0.0252
	10.1816	1.0006	0.0516
	15.2011	1.0001	0.0770
0.3010	5.0698	1.0001	0.0235
	10.1171	1.0002	0.0469
	15.1186	1.0004	0.0701
0.3300	5.0086	1.2946	0.0292
	9.9686	0.9534	0.0428
	14.9744	1.0158	0.0685
0.4000	5.1425	1.0163	0.0218
	10.4780	0.9930	0.0434
	15.0708	0.9974	0.0627
0.4599	5.2913	1.0163	0.0208
	9.9457	0.9956	0.0383
	15.0469	1.0292	0.0599
0.4850	5.0851	1.0265	0.0195
	10.0104	1.0108	0.0378
	15.0464	0.9945	0.0559
0.5003	5.0066	0.9236	0.0169
	9.9476	1.0122	0.0368
	14.9910	1.0075	0.0552
0.5500	5.0534	1.0140	0.0173
	9.9904	0.9932	0.0335
	15.1872	1.0200	0.0523
0.6000	4.9334	1.0850	0.0165
	10.8325	0.9793	0.0327
	14.9945	0.9909	0.0458
0.6702	5.0084	1.1254	0.0149
	9.9531	1.0642	0.0280
	14.9787	1.1390	0.0451
0.7000	4.9872	1.0007	0.0122
	10.0159	1.0088	0.0247
	14.9892	1.0316	0.0378
0.7500	20.0985	1.5776	0.0665
	25.0253	0.9012	0.0473
	29.9764	0.9305	0.0585

left on the balance, and tepo was added (ca. 5 mol % per 1 mol of [C_8mim]$^+$ cation; see Table 3 for the accurate masses). This was repeated for solutions containing 10 and 15 mol % of tepo per 1 mol of [C_8mim]$^+$ cation.

Typically, a sample vial was closed with a plastic cap, and the mixture was stirred overnight at 80 °C to ensure full dissolution. Subsequently, the liquid was loaded into an NMR tube (5 mm, borosilicate glass), containing a sealed capillary with dimethyl-d_6 sulfoxide (an external lock). The tube was closed with a standard cap, sealed with parafilm, and removed from the glovebox immediately prior to measurement.

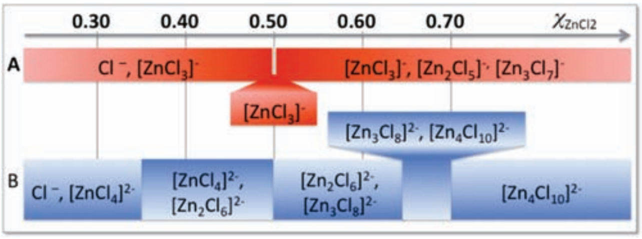

Figure 1. Two contrasting models, A and B, illustrating the major anions purported to be present in chlorozincate(II) systems as a function of their composition, χ_{ZnCl_2}.[28−33]

^{31}P NMR spectra were acquired at 121.452 MHz using a Bruker DRX 300 spectrometer. Phosphoric(V) acid, an 85% solution in water, was used as an external reference. All samples were measured at 27 °C. Moreover, the three solutions of tepo in hexane (ca. 5, 10, and 15 mol %) were prepared and then measured. From the ^{31}P NMR chemical shifts measured for tepo in hexane, the ^{31}P NMR chemical shift for infinite dilution, δ_{inf}, was determined by extrapolation, and all other chemical shifts are reported relative to this value.[2,36]

■ RESULTS AND DISCUSSION

Critical Review of the Extant Literature. Several groups have used a wide range of analytical techniques in an attempt to determine the anionic speciation of chlorozincate(II) ionic liquids, deducing the speciation patterns summarized in Figure 1A.[28−31] In contrast, Alves et al.[32] published a Raman spectroscopic study of the [C_4mim]Cl−$ZnCl_2$ system, followed by a detailed DSC investigation,[33] proposing an alternative speciation, as shown in Figure 1B. Thus, there are two diametrically opposed models for the speciation of zinc(II) chloride ionic liquids, where the only common anion claimed is the chloride ion.

Discussion of the Speciation Techniques. The published studies on the speciation of chlorozincate(II) ionic liquids are summarized in Table 4.

The principal feature to emerge from a brief examination of this table is that the majority of studies have aligned behind model A (as shown in Figure 1). However, a closer examination reveals that the experimental studies that led to these conclusions were conducted under extremely different conditions, even in different states, e.g., an ionized gas phase, a neat liquid, a solution, or a solid state. Despite that, the deductions from these studies were assumed to be related directly to the speciation in the neat ionic liquid (in the liquid state). A question arises, should the species present in different states, a priori, be the same, or does the speciation depend ultimately on the state of matter of the analyzed sample? The answer to this question has been established many times, in many systems, and it is incontrovertable that the structure is state-dependent.[38]

The first paper describing the speciation of chlorozincate(II) ionic liquids was that of Lin et al.,[25a] which mainly focused on the electrodeposition of zinc; it suggested the presence of [$ZnCl_4$]$^{2-}$ or coordinationally unsaturated chlorozincate(II) species such as [$ZnCl_3$]$^-$, without giving any experimental evidence to support either model A or model B (Figure 1).

Subsequently, Hsiu et al.[30] investigated the speciation of the [C_2mim]Cl−$ZnCl_2$ system. Using fast atom bombardment mass

Table 4. Speciation of Chlorozincate(II) Ionic Liquids According to the Published Literature: Analytical Techniques, Phase of the Tested Samples, and Deduced Speciation

speciation technique	phase	model	ref
FAB-MS	ionized gas	A	14, 18, 29
ESI-MS	ionized gas	A	28
Raman	neat liquid	B	31
^{1}H and ^{13}C NMR	solution	A	28
^{35}Cl NMR	neat supercooled liquid	A	28
solid-state ^{1}H and ^{13}C NMR	neat solid	A	28
single-crystal X-ray diffraction	neat solid	B	37
powder X-ray diffraction	neat solid	A	27
EXAFS	neat solid or liquid	A	30
XANES	neat solid or liquid	A	30
cyclic voltammetry	neat liquid	A	14, 29
freezing point[a]	neat solid/liquid	A	14
DSC	neat solid/liquid	B	32
DSC	neat solid/liquid	A	27, 28, 30
POM	neat solid	A	27

[a] Determined by the lack of flow in the meniscus.

Table 5. Peaks Found in Positive, ESI(+), and Negative, ESI(−), Mode Mass Spectra of the $[C_8mim]Cl-ZnCl_2$ System (Solution in Ethanenitrile) and Corresponding Cationic and Anionic Species

ESI(+)		ESI(-)	
m/z[a]	assignment	*m/z*[a]	assignment
195	$[C_8mim]^+$	171	$[ZnCl_3]^-$
425	$[(C_8mim)_2Cl]^+$	265	$[(C_8mim)Cl_2]^-$
791	$[(C_8mim)_3ZnCl_4]^+$	309	$[Zn_2Cl_5]^-$
		444	$[Zn_3Cl_7]^-$
		497	$[(C_8mim)_2Cl_3]^-$
		539	$[(C_8mim)Zn_2Cl_6]^-$
		633	$[(C_8mim)_2ZnCl_5]^-$
		727	$[(C_8mim)_3Cl_4]^-$
		863	$[(C_8mim)_3ZnCl_6]^-$
		958	$[(C_8mim)_4Cl_5]^-$
		1095	$[(C_8mim)_4ZnCl_7]^-$
		1188	$[(C_8mim)_5Cl_6]^-$
		1326	$[(C_8mim)_5ZnCl_8]^-$
		1420	$[(C_8mim)_6Cl_7]^-$

[a] *m/z* values quoted represent the most intense peak in each multiplet; full details are given in the Supporting Information.

spectrometry (FAB-MS), a gas-phase technique,[39] they proposed a speciation in the liquid state (model A)[30] analogous to that of well-known chloroaluminate(III) ionic liquids.[5,40] Noteworthy, although no $[ZnCl_4]^{2-}$ was found in the basic régime using mass spectrometry (ionized gas phase), they observed by cyclic voltammetry (neat ionic liquid) that the limit of free chloride anion presence is $\chi_{ZnCl_2} \leq 0.33$, which implies the formation of $[ZnCl_4]^{2-}$ and, hence, points toward model B. Subsequently, different groups also supported the speciation shown in model A using mass spectrometry (FAB-MS and ESI-MS).[14,18,29,30]

Studies on solids, viz., solid-state NMR experiments (^{1}H and ^{13}C)[29] and powder X-ray diffraction, combined with polarized optical microscopy (POM) images,[28] again concluded that the speciation in the *liquid phase* follows model A. In addition, solution NMR studies (^{1}H and ^{13}C)[29] were carried out; however, such tests cannot possibly reveal direct structural information about the speciation of an inorganic anion.

Turning to the neat ionic liquid state, DSC studies are often used to produce phase diagrams, a useful, although indirect, tool for the speciation of chlorometallate ionic liquids.[11,8,41] However, the early DSC investigations,[28,29,31] despite the fact that they had far too few points to allow the construction of a detailed phase diagram, were interpreted in favor of model A, which at that point was the preferred model in the literature. In a more recent study,[31] extended X-ray absorption fine structure (EXAFS) and X-ray absorption near-edge structure (XANES) data were published. Although structural techniques, these methods are considered as "sporting" ones,[42] because "comparison with standard materials and the use of EXAFS in conjunction with other techniques to ensure a realistic interpretation of the data are vital."[43] Analysis of the reported data[31] is transparently flawed and, *pace* the conclusions of Zou et al.,[31] it will not allow discrimination between model A and model B.

In 2008, the first direct spectroscopic probe of the anionic speciation was published. Alves et al.[32] used Raman spectroscopy to study the neat liquid $[C_4mim]Cl-ZnCl_2$ system. The bands characteristic of chlorozincate(II) anions were compared to the rich literature data available on classical chlorozincate(II) molten salts. These spectroscopic analyses on the liquid state led to the first proposal of model B and were incompatible with the speciation of model A. A more recent development[33] (a DSC study, from some of the same authors) resulted in a phase diagram in which the key features correspond to the previously observed speciation from the Raman study (model B).

Thus, to summarize, two models for the anionic speciation in the liquid chlorozincate(II) systems are presented in the literature (Figure 1). The dominant model, model A, supports the presence of monocharged chlorozincate(II) anions, in analogy to chloroaluminate(III) systems. The less popular model, model B, suggests the existence of doubly charged chlorozincate(II) species, in accord with the known coordination chemistry of classical chlorozincate(II) salts in the molten state.[44] Consequently, an independent arbitration between these models is necessary. In this paper, we present new experimental data, compare and integrate with data from the literature, and attempt to resolve which model is correct.

Synthesis of the $[C_nmim]Cl-ZnCl_2$ Systems. Chlorozincate(II) compositions based on the $[C_8mim]^+$ cation were pale-yellow, very viscous liquids, whereas those based on the $[C_2mim]^+$ cation were crystalline or glass. For $\chi_{ZnCl_2} > 0.75$, homogeneous liquids were not obtained, and an insoluble white powder was observed.

The $[C_8mim]^+$ systems were chosen in order to obtain a wide liquid range, in contrast to, for example, the $[C_2mim]^+$ system, where higher melting solids were formed.

Mass Spectrometry of the $[C_nmim]Cl-ZnCl_2$ Systems. A range of samples of the $[C_8mim]Cl-ZnCl_2$ system ($0.25 \leq \chi_{ZnCl_2} \leq 0.75$) were tested using ESI-MS. All of the species found in both positive, ESI(+), and negative, ESI(−), modes are listed in Table 5. Importantly, there was no evidence for coordination of the electrospray solvent (ethanenitrile) to zinc, irrespective of χ_{ZnCl_2}.

For all tested compositions, the most intense peak in the positive mode corresponded to the molecular peak of the cation, $[C_8mim]^+$ (*m/z* 195). All other peaks were of extremely low

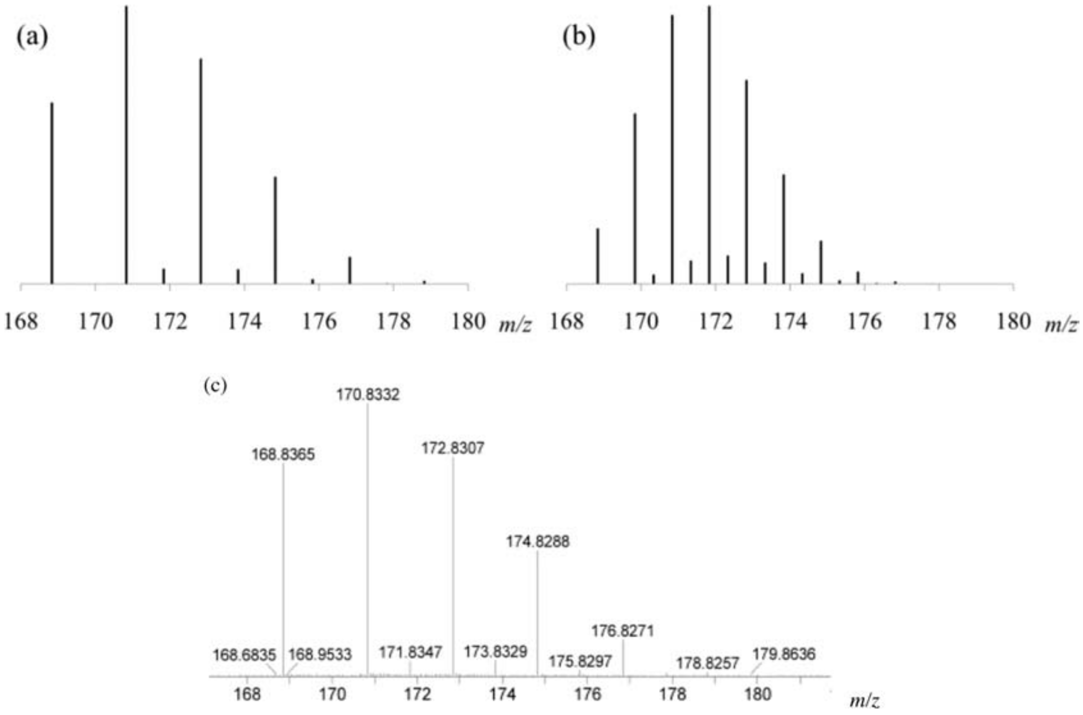

Figure 2. ESI-MS molecular peaks for (a) $[ZnCl_3]^-$, simulated;[45] (b) $[Zn_2Cl_6]^{2-}$, simulated;[45] and (c) $[ZnCl_3]^-$, experimental from this work.

intensity, with the $[(C_8mim)_3ZnCl_4]^+$ (m/z 791) cluster found in all spectra and traces of the $[(C_8mim)_2Cl]^+$ (m/z = 425) cluster present only for χ_{ZnCl_2} = 0.25 and 0.33.

In the negative mode, for all compositions, the most intense peak was m/z 171, corresponding to the $[ZnCl_3]^-$ anion. It is important to note that the isotopic pattern of this peak corresponds to the presence of three chloride anions and not to the presence of the dimer, $[Zn_2Cl_6]^{2-}$, as illustrated in Figure 2. Moreover, there was no evidence for any other dipositive or dinegative ions in the mass spectra recorded. The second most intense set of peaks in each spectrum corresponded to $[Zn_3Cl_7]^-$ (m/z 444); the intensity of this multiplet increased markedly with increasing χ_{ZnCl_2}. The dinuclear anion, $[Zn_2Cl_5]^-$, was also detected in each case, but the corresponding signals (m/z 309) were always far less intense than those corresponding to $[Zn_3Cl_7]^-$.

As shown in Table 5, a wide range of high-m/z clusters was observed in the negative mode. These could be divided into two categories: clusters comprised of cations and chloride, of the general formula $[(C_8mim)_xCl_{x+1}]^-$, x = 1−6, and clusters incorporating cations, chlorine, and zinc, $[(C_8mim)_xZnCl_{x+3}]^-$, x = 3−6, and also $[(C_8mim)Zn_2Cl_6]^-$. It is noteworthy that all signals were found in all of the tested samples ($0.25 \le \chi_{ZnCl_2} \le 0.75$) but also that the relative intensities of the listed peaks changed with the composition. As expected, with increasing χ_{ZnCl_2}, the intensity of the former ions (without zinc) decreased and the intensity of the latter type (containing zinc) increased.

The outcome of the ESI-MS experiments (vide supra) was in agreement with the results obtained by other groups; the same chlorozincate(II) species were observed using both ESI-MS[29] (samples tested as solutions in ethanenitrile) and FAB-MS (experiments with use of either a matrix or a neat ionic liquid).[18,14,30] The widest range of chlorozincate(II) compositions has been analyzed by Lecocq et al.;[29] using ESI-MS, they found only $[ZnCl_3]^-$ in $\chi_{ZnCl_2} \le 0.50$ samples, and all three chlorozincate(II) anions: $[ZnCl_3]^-$, $[Zn_2Cl_5]^-$, and $[Zn_3Cl_7]^-$ in $\chi_{ZnCl_2} > 0.50$ compositions. However, in our work, all three chlorozincate(II) species were found in each sample, regardless of the composition, but in different relative proportions. Furthermore, the high-m/z (>490) clusters (see Table 5), mentioned by Lecocq et al.[29] to be of very low intensity appeared in this work to constitute a significant part of the anionic speciation found by ESI-MS, even if their signals were weaker than those related to $[Zn_xCl_y]^-$ anions.

As demonstrated above, the identity of the species present, based on ESI-MS, was insensitive to the composition; polynuclear $[Zn_xCl_y]^-$ species were detected even for a very low content of zinc(II) chloride (χ_{ZnCl_2} = 0.25), while the chloride-containing complexes, $[(C_8mim)_xCl_{x+1}]^-$, were found for samples where no free chloride would be expected (χ_{ZnCl_2} = 0.75). Moreover, the large anionic clusters, detected in all samples, were never reported to be present, as discrete species, in the liquid phase in any ionic liquid. At the same time, such clusters, as well as a number of other species observed in the mass spectra but not in the liquid phase, have been well described in the literature (see, for example, the review by Kebarle[46]).

In ESI-MS, there are several stages of transfer of ions in solution to ions in the gas phase:[39] (i) production of a charged droplet of the solution, (ii) shrinkage of the droplet (solvent evaporation) and numerous subsequent fisions of the droplet to produce very small droplets of high charge, and (iii) production of gas-phase ions from the small droplets. These stages are followed by secondary processes, involving modification of the gas-phase ions. The mechanism of the production of gas-phase ions and their subsequent reactions will affect the speciation observed in the mass spectrum. For example, a similar problem has been encountered by Di Marco et al.,[47−50] who devoted a number of publications to studies of metal−ligand aqueous solution equilibria using ESI-MS. They stated that "the correlation between conditions in solution and mass spectra in the gas phase is far from being completely established"[47] and that "the ionization process can introduce perturbations which affect the speciation results in an unpredictable way".[50] By modification of the instrumental parameters, they identified a range of such perturbations, including gas-phase reactions and thermal decomposition of ions.[49,50] In their recent work, Di Marco et al.[50] postulated that such phenomena are both chemistry- and instrument-dependent and that "the identification of perturbations is a required task for any metal−ligand equilibrium study performed by ESI-MS".[50] This raises the question as to whether ESI-MS results, which are measured in the gas phase, correspond to the actual species present in the liquid phase. Kebarle[46] gives a clear answer: "the ions observed in the gas phase may be different from those present in the solution, owing to processes which occur at the threshold between solution and gas phase and ion−molecule reactions in the gas phase".

The same problem applies to FAB-MS, with additional uncertainty regarding the actual phase of the tested sample. The more recent opinions point toward either the gas phase,[51] the predominant role of the gas phase,[52] or a hybrid "bubble chamber model".[53] The fact that the anions found (with or without a matrix) in FAB-MS[18,14,30] were identical with those observed in ESI-MS points toward the gas phase, which is an interesting matter for further investigation but reaches far outside the scope of this paper. Nevertheless, it is worth mentioning that there are hundreds of papers in the literature using mass spectrometry to investigate ionic liquids.[54] In the past, a number of publications,[11c,55] including some from our group,[56] relied heavily on FAB-MS to study chlorometallate ionic liquid systems, and therefore these results should be revisited.

Because it is obvious that the mass spectrometric speciation cannot be directly translated to the liquid phase, it seemed far more reasonable to probe the structure using direct spectroscopic techniques on neat ionic liquids.

Raman Spectroscopy of the [C_8mim]Cl−$ZnCl_2$ System. Raman spectra of the neat liquid samples of the [C_8mim]Cl−$ZnCl_2$ system, for six different compositions, are shown in Figure3.

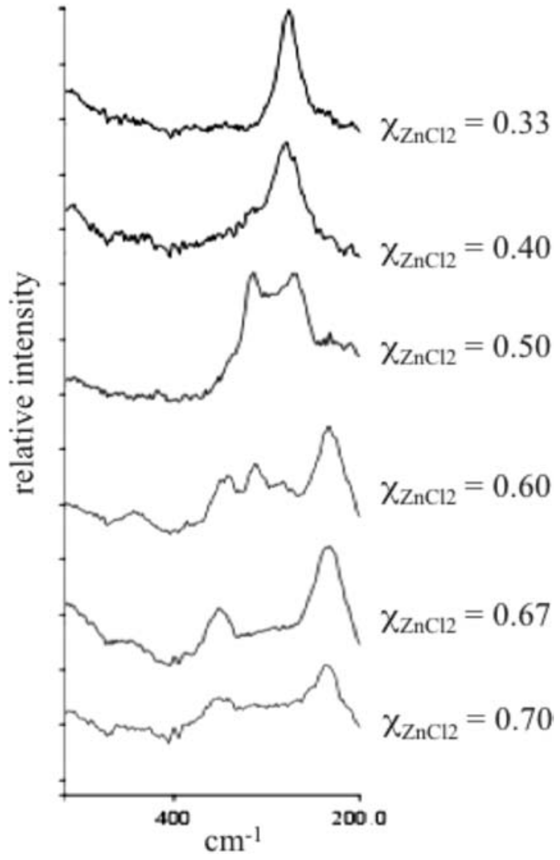

Figure 3. Raman spectra of the [C_8mim]Cl−$ZnCl_2$ system, where the χ_{ZnCl_2} values are quoted.

The wavenumbers for the major vibrations characteristic of ZnCl are listed in Table 6.

For χ_{ZnCl_2} = 0.33, the only strong peak in the region 200−400 cm^{-1} was observed at 275 cm^{-1}. This can be ascribed to tetrahedral $[ZnCl_4]^{2-}$ anions, which are well described in the literature, with a $\nu_1(a_1)$ vibration at a wavelength of 282 cm^{-1} (for an aqueous solution of the cesium salt).[57] Moreover, a single crystal of $[C_2mim]_2[ZnCl_4]$ has been obtained from the χ_{ZnCl_2} = 0.33 composition (see Figure 9). This salt has been characterized using Raman spectroscopy, and the $\nu_1(a_1)$ vibration of $[ZnCl_4]^{2-}$ has been observed at 280 cm^{-1}. Thus, the peak at 275 cm^{-1} unambigously characterizes the T_d structure of $[ZnCl_4]^{2-}$. To our knowledge, there is no structural or spectroscopic evidence for the existence of $[ZnCl_3]^-$ in either the solid or liquid state.

As the composition of the [C_8mim]Cl−$ZnCl_2$ system becomes more acidic, the $\nu_1(a_1)$ band from $[ZnCl_4]^{2-}$ remains visible at χ_{ZnCl_2} = 0.4, with a minimal shift to 278 cm^{-1}, but a shoulder starts to appear at 312 cm^{-1}. The latter peak becomes much more intense for an equimolar mixture of [C_8mim]Cl and $ZnCl_2$. In a study of a $ZnCl_2$−(Li,K)Cl system, Babushkina and Volkov[58] assigned a peak at 292 cm^{-1} to $[Zn_2Cl_6]^{2-}$, but the spectra were of poor quality. Later, Yannopoulos et al.[59] studied molten zinc(II) chloride and, in the high-temperature chloride melt, observed a peak at 300 cm^{-1}, ascribing it to dimeric $\{Zn_2Cl_6\}^{2-}$ units within the overall polymeric structure. Thus, there is not a good comparator for the hexachlorodizincate(II)

Table 6. Raman Frequencies (cm^{-1})[a] of the Chlorozincate(II)-Related Peaks Obtained for Different Compositions of [C_8mimCl]Cl−$ZnCl_2$

	χ_{ZnCl_2}					
assignment	0.33	0.40	0.50	0.60	0.67	0.70
$[ZnCl_4]^{2-}$	275 (s)	278 (s)				
$[Zn_2Cl_6]^{2-}$		312 (sh), 269 (sh)	312 (s), 269 (s)	312 (m)		
$[Zn_3Cl_8]^{2-}$				340 (m), 288 (m)		
$[Zn_4Cl_{10}]^{2-}$				348 (sh), 232 (s)	348 (m), 232 (s)	348 (m), 232 (s)

[a] The intensities of the peaks are represented in parentheses (s = strong, m = medium, and sh = shoulder).

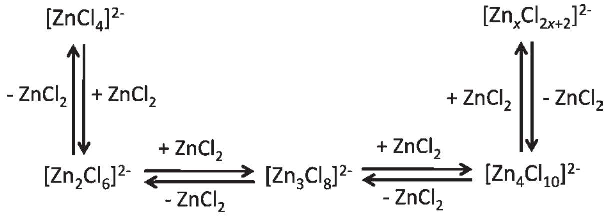

Figure 4. Equilibria between chlorozincate(II) anions in the liquid phase of the $[C_8mim]Cl-ZnCl_2$ system, based on Raman spectroscopy.

anion in the literature, although it may be expected that the $Zn-Cl_{terminal}$ stretching frequency would be greater than that of tetrachlorozincate(II). Fortunately, the crystal strucure of $[C_2mim]_2[Zn_2Cl_6]$ has been determined (see Figure 9c), with its Raman bands occurring at 264 and 317 cm^{-1}. Consequently, the peaks at 269 and 312 cm^{-1} can be ascribed to a doubly charged $[Zn_2Cl_6]^{2-}$ anion.

Moving further toward the acidic régime, for the $\chi_{ZnCl_2} = 0.60$ sample, the signals for the $[ZnCl_4]^{2-}$ anion disappear, whereas the peak at 312 cm^{-1} (assigned to $[Zn_2Cl_6]^{2-}$) remains. Furthermore, two new pairs of peaks were found: at 288 and 340 cm^{-1} and at 232 and 348 cm^{-1}. For more acidic compositions ($\chi_{ZnCl_2} = 0.67$ and 0.70), only two peaks out of five remained: $\nu = 232$ and 348 cm^{-1}. Considering this, one can assume that the two pairs of peaks in the $\chi_{ZnCl_2} = 0.60$ composition originate from two different polynuclear species.

In their study, Yannopoulos et al.[59] calculated the vibrational wavelength of a $\{Zn(Cl_{2/2}Cl_2)\}^-$ species to be 355 cm^{-1}, corresponding to the $Zn-Cl_{terminal}$ stretching frequencies in the trimeric and/or tetrameric anions from model B. Therefore, both peaks at 340 and 348 cm^{-1} can be assigned to such complexes. The band at 288 cm^{-1} (found only for $\chi_{ZnCl_2} = 0.60$) can be assigned to the $\nu_1(e)$ vibration of the $(Zn_2Cl_2Cl_{4/2})$-Zn pattern,[59] corresponding to $Zn-Cl_{bridging}$ in the linear trinuclear anion, $[Zn_3Cl_8]^{2-}$, described in model B. Moreover, the $\nu_{terminal}/\nu_{bridging}$ ratio, 288/340, is 0.84, which falls within the limits 0.60−0.85, normally found for the ratio of a bridging metal−halogen stretching frequency to a terminal metal−halogen stretching frequency.[60] Considering the stoichiometry, it is logical to ascribe the peaks at 288 and 340 cm^{-1} to a linear trimeric structure, $[Zn_3Cl_8]^{2-}$. The band at 232 cm^{-1} (found in all acidic compositions) has been described to represent the bridging vibrations in $(ZnCl_{4/2})Zn$ with a central tetrahedral zinc.[59] Thus, the pair of peaks present in the most acidic régime ($\nu = 232$ and 348 cm^{-1}) may represent a nonlinear chlorozincate(II) anion of the molecular formula $[Zn_4Cl_{10}]^{2-}$ and also, according to stoichiometry, other polynuclear species, $[Zn_xCl_{2x+2}]^{2-}$.

In the Raman spectra of the six compositions of $[C_8mim]Cl-ZnCl_2$, all of the observed bands could be rationalized in terms of the following equilibria (Figure 4):

Thus, as zinc(II) chloride is added to the system, making it more acidic, the above equilibria shift from left to right, following model B.

Lewis Acidity of the $[C_8mim]Cl-ZnCl_2$ System. AN is a well-established quantitative measure of Lewis acidity[61] and has been used to quantify the Lewis acidity of some chloroaluminate(III) systems[62] and, more recently, also for chlorogallate(III) and chloroindate(III) ionic liquids.[2] A probe, tepo, was introduced into the neat liquid, and its chemical shift was measured using ^{31}P NMR spectroscopy. To obtain precise measurements, as advised by Gutmann,[36] the ^{31}P NMR chemical shifts were measured at several concentrations of tepo, and the data were extrapolated to infinite dilution, from which a value of δ_{inf} (^{31}P chemical shift at infinite dilution of tepo) could be deduced. The AN value is calculated, as shown in eq 1.[36]

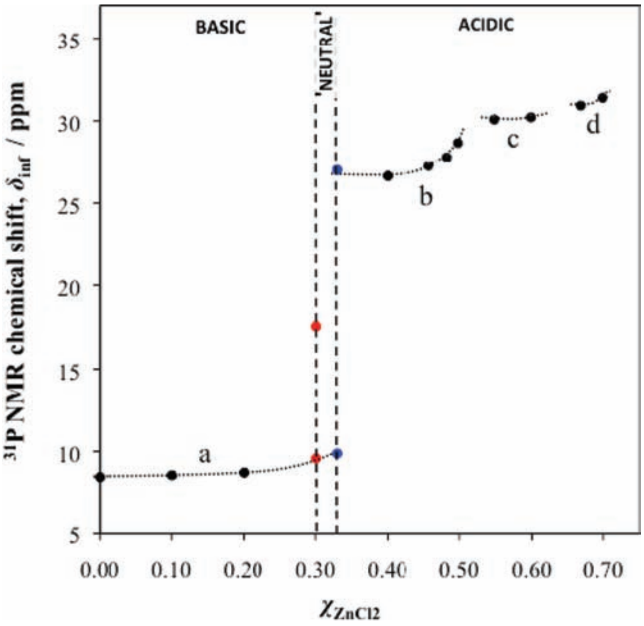

Figure 5. Plot of the ^{31}P NMR shifts of tepo solutions at infinite dilution, δ_{inf}, in the $[C_8mim]Cl-ZnCl_2$ system. Each pair of colored points represents a single composition; the dotted lines are only visual guides.

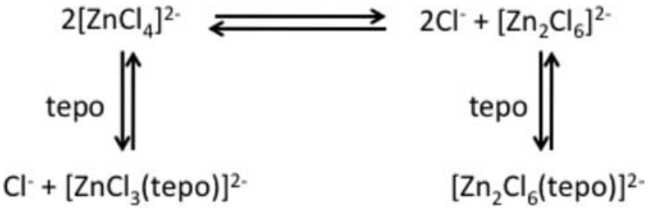

Figure 6. Equilibria between mononuclear and dinuclearzinc(II) complexes in the $[C_8mim]Cl-ZnCl_2$ system, in the presence of added tepo.

$$AN = 2.348\delta_{inf} \qquad (1)$$

By definition, the value of AN for hexane has been assigned to zero and that for antimony(V) chloride (10^{-3} M solution in 1,2-dichloroethane) to 100.

In this work, a range of samples of the $[C_8mim]Cl-ZnCl_2$ system were tested; ^{31}P NMR chemical shifts for infinite dilution of tepo, δ_{inf}, were plotted against the composition, χ_{ZnCl_2} (see Figure 5). For all but two compositions, a single peak was found in the ^{31}P NMR spectra. For $\chi_{ZnCl_2} = 0.30$ and 0.33, two peaks were observed, indicating that there were two independent tepo−chlorozincate(II) complexes present, not exchanging on the NMR time scale.

For $0 < \chi_{ZnCl_2} < 0.33$ (Figure 5, region a), the δ_{inf} values vary only slightly and then rise dramatically at around $\chi_{ZnCl_2} = 0.33$. Within the $0.33 < \chi_{ZnCl_2} < 0.50$ range (Figure 5, region b), the δ_{inf} values increase almost exponentially with increasing χ_{ZnCl_2}. Beyond $\chi_{ZnCl_2} = 0.50$, the change in δ_{inf} is far less dramatic, with

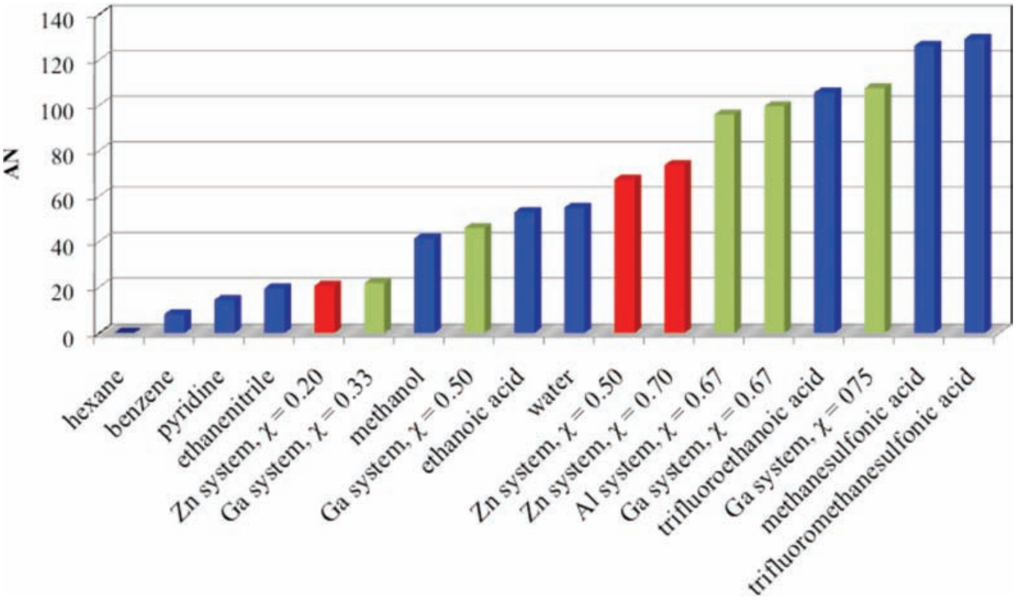

Figure 7. Comparison of ANs of selected compositions of the $[C_8mim]Cl-ZnCl_2$ system (this work, red), some 1-octyl-3-methylimidazolium chlorometallate(III) systems (green),[2] and common solvents and acids (blue).[36].

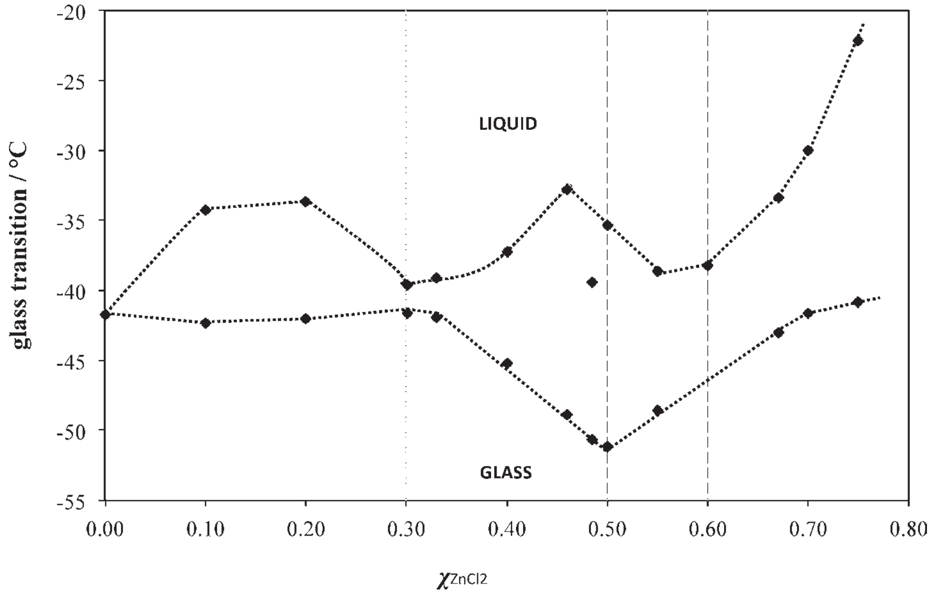

Figure 8. Phase diagram of the $[C_8mim]Cl-ZnCl_2$ system, based on glass transition temperatures. The dotted lines are only visual guides.

a plateau for $0.50 < \chi_{ZnCl_2} < 0.60$ (Figure 5, region c) and a mild increase for $0.67 < \chi_{ZnCl_2} < 0.70$ (Figure 5, region d).

Low δ_{inf} values for $\chi_{ZnCl_2} < 0.33$ correspond to the presence of the Lewis basic chloride anion in equilibrium with the coordinationally saturated $[ZnCl_4]^{2-}$ species. At $\chi_{ZnCl_2} > 0.33$, the chloride anion is entirely consumed, and a Lewis acidic dimer, $[Zn_2Cl_6]^{2-}$, is formed; its concentration increases with an increase in χ_{ZnCl-}, which is reflected in an increasing value of δ_{inf}. This change between the Lewis acidic and Lewis basic compositions around the theoretical neutral point ($\chi_{ZnCl_2} = 0.33$) is obviously the most pronounced change observed in Figure 5.

A theoretically neutral composition was expected at $\chi_{ZnCl_2} = 0.33$, with $[C_8mim]_2[ZnCl_4]$ present as the only compound (see Raman studies; Figure3). However, rather than a distinctive neutral point, a "neutral zone" was found between $\chi_{ZnCl_2} = 0.30$ and 0.33, with two ^{31}P NMR signals for each of the two compositions. In both cases, one of the signals corresponded to the Lewis basic δ_{inf} values, and the other one was shifted toward a more acidic region (see Figure 5). Of course, it is known that the preparation of an exactly neutral composition in chlorometallate systems is extremely difficult.[63] Nevertheless, two peaks were found in two samples and not in a "borderline" composition. Seemingly (in contrast to, e.g., chloroluminate(III) systems), the central equilibrium in Figure 6 has a relatively low equilibrium constant, with all three anions, Cl^-, $[ZnCl_4]^{2-}$, and $[Zn_2Cl_6]^{2-}$, present in the $\chi_{ZnCl_2} = 0.30-0.33$ region in

Table 7. Crystallographic Details for the Crystal Structures of the Compounds $[C_2mim]_2[ZnCl_4]$, $[C_2mim]_2[Zn_2Cl_6]$, and $[C_2mim]_2\{Zn_4Cl_{10}\}$

	$[C_2mim]_2[ZnCl_4]$	$[C_2mim]_2[Zn_2Cl_6]$	$[C_2mim]_2\{Zn_4Cl_{10}\}$
formula	$C_{12}H_{22}Cl_4N_4Zn$	$C_{12}H_{22}Cl_6N_4Zn_2$	$C_{12}H_{12}Cl_{10}N_4Zn_4$
MW/g	429.51	565.78	828.24
dimensions/mm	0.22 × 0.12 × 0.03	0.4 × 0.38 × 0.18	0.18 × 0.11 × 0.05
cryst syst	tetragonal	monoclinic	monoclinic
space group	$I4_1/a$(No. 88)	$P2_1/n$ (No. 52)	$C2$ (No. 5)
a/Å	14.0059(3)	7.71750(10)	16.6552(4)
b/Å	14.0059(3)	17.1624(5)	9.2453(2)
c/Å	19.1380(8)	8.8476(2)	17.9079(4)
α/deg	90.00	90.00	90.00
β/deg	90.00	109.393(2)	107.508(1)
γ/deg	90.00	90.00	90.00
V/Å^3	3754.21(19)	1105.38(4)	2629.76(10)
Z	8	4	4
D_{calc}/g cm^{-3}	1.530	3.400	2.092
cryst shape	plate	block	plate
cryst color	colorless	colorless	colorless
μ/mm^{-1}	1.876[a]	5.796[a]	4.631[a]
F(000)	1760	1136	1608
measd reflns	12 275	13 928	11 623
unique reflns	2152	2531	5840
parameters refined	117	111	238
GOF on F^2	1.149	1.389	0.990
R1	0.0383	0.0220	0.0315
wR2	0.0704	0.0680	0.0788
R1 (all data)	0.0546	0.0284	0.0415
wR2 (all data)	0.0779	0.0923	0.0920
CCDC	816796	816797	816798

[a] Mo Kα radiation.

significant amounts. Because $[Zn_2Cl_6]^{2-}$ was not observed by Raman spectroscopy, it must be present at a low concentration. The reaction of tepo with coordinatively saturated $[ZnCl_4]^{2-}$ would be displacement of a chloride ion, whereas the reaction with $[Zn_2Cl_6]^{2-}$ would be an addition via cleavage of the Zn−Cl$_{bridging}$ bond.

For $\chi_{ZnCl_2} > 0.50$ compositions, only polynuclear species are present, and further regions (c and d) in Figure 5 correspond to the appearance of the polynuclear Lewis acidic species $[Zn_3Cl_8]^{2-}$ and $[Zn_4Cl_{10}]^{2-}$. The δ_{inf} values change only slightly because the reaction of tepo with such polynuclear anions is of the same nature as the reaction with $[Zn_2Cl_6]^{2-}$ (see Figure 6), an addition with cleavage of a Zn−Cl$_{bridging}$ bond.

The observed pattern of acceptor properties, with a dramatic change at $\chi_{ZnCl_2} = 0.33$, is in agreement with the Raman spectroscopic studies (Figure3) and supports strongly model B.

In order to get a perspective on the Lewis acidity of the chlorozincate(II) system, AN values calculated for the $[C_8mim]Cl-ZnCl_2$ system were compared with the values found for other chlorometallate systems,[2] as well as with common molecular solvents and acids[36] (Figure 7).

Whereas the $\chi_{ZnCl_2} = 0.20$ composition is basic, with a very low AN value, similar to basic chlorogallate(III) ionic liquids and to ethanenitrile, the $\chi_{ZnCl_2} = 0.50$ ionic liquid is Lewis acidic, with an AN number of over 12 units higher than that of water. The increase in acidity between $\chi_{ZnCl_2} = 0.50$ and 0.70 is rather small, and the Lewis acidities of all chlorozincate(II) systems are significantly lower than that of the chlorogallate(III) or chloroaluminate(III) systems, as expected. These conclusions are in agreement with the catalytic applications of chlorozincate(II) systems, wherein they are used as mild Lewis acidic catalysts.[19−21]

Phase Transitions of the $[C_8mim]Cl-ZnCl_2$ System. All phase transitions, plotted in Figure 8, detected in the DSC scans (−90 to +40 °C) of the $[C_8mim]Cl-ZnCl_2$ system were second-order transformations (glass transitions, T_g). T_g data are usually less reproducible than melting points; however, here the descrepancy between the values (for six different compositions tested in duplicate) was always within ±1 °C. For all but one composition ($\chi_{ZnCl_2} = 0.60$), two transitions were found in each DSC scan.

Because the phase diagram is based on glass transitions and not on melting points, it would be incorrect to discuss it in terms of eutectic or peritectic points. Nevertheless, there are distinct maxima and minima in Figure 8 ($\chi_{ZnCl_2} = 0.33$, 0.50, and 0.60) that correspond approximately to the speciation detected with Raman spectroscopy (Figure3) and to the acceptor property data (Figure 5, regions a−d).

Instead of sharp transitions for $\chi_{ZnCl_2} = 0.33$, 0.50, 0.60, and 0.67, where single compounds might have been expected based on stoichiometry, one or two glass transitions were found. Glass transitions were observed despite the presence of doubly charged

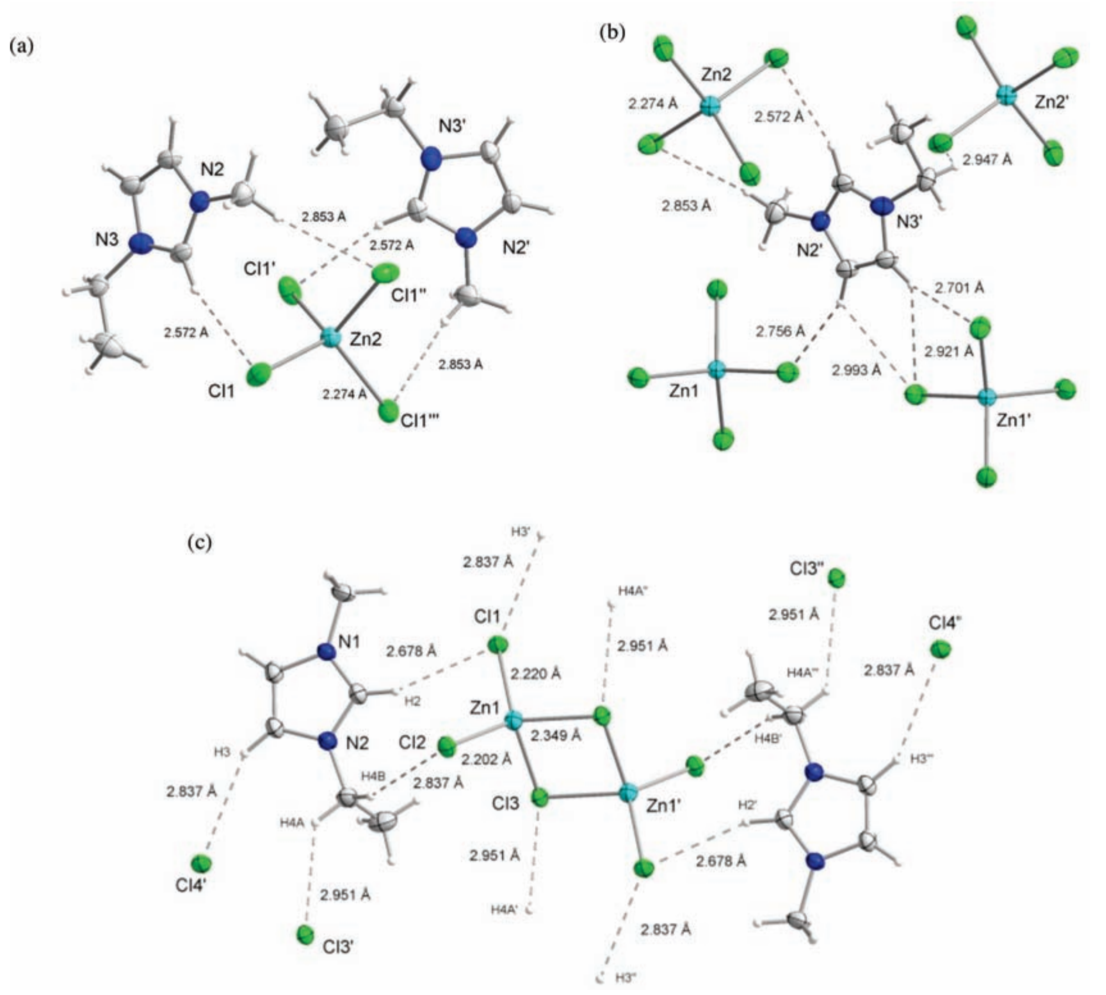

Figure 9. Crystal structures of (a) $[C_2mim]_2[ZnCl_4]$, obtained for $\chi_{ZnCl_2} = 0.33$, (b) the cation surrounding for the structure of $[C_2mim]_2[ZnCl_4]$, and (c) $[C_2mim]_2[Zn_2Cl_6]$, obtained for $\chi_{ZnCl_2} = 0.50$.

anions that might have been expected to lead to crystallization. It is known from other chlorometallate systems, e.g., $[C_2mim]Cl-AlCl_3$,[41] that glass formation is favored when there are dynamic equilibria between a multiplicity of anions.

Crystallography. Because all of the phases of the $[C_8mim]Cl-ZnCl_2$ system were liquid at room temperature, it was decided to investigate a system with a similar, but significantly smaller, cation and a much more rigid side chain. The $[C_2mim]Cl-ZnCl_2$ system was chosen, and an attempt was made to obtain crystal structures at each of the significant compositions.

Directly after the preparation and subsequent rapid cooling to room temperature, all samples of the $[C_2mim]Cl-ZnCl_2$ system were supercooled glasses. Crystals of $\chi_{ZnCl_2} = 0.33$ and 0.50 compositions, of a quality suitable for the X-ray diffraction experiments, were obtained by cooling the samples very slowly (48 h, from 120 °C to ambient temperature). Furthermore, crystals of the $\chi_{ZnCl_2} = 0.75$ composition were formed after storing the sample in a freezer (24 h, −25 °C) and subsequently conditioning it at room temperature (24 h). Despite numerous attempts, it did not prove possible to crystallize two other compositions ($\chi_{ZnCl_2} = 0.60$ and 0.67). Importantly, whereas for $\chi_{ZnCl_2} = 0.33$ and 0.50, all of the samples turned into crystalline materials upon standing at room temperature, for the $\chi_{ZnCl_2} = 0.75$ composition, only a small number of crystals were formed despite a prolonged time of crystallization.

Crystal structures obtained were $[C_2mim]_2[ZnCl_4]$ from $\chi_{ZnCl_2} = 0.33$, $[C_2mim]_2[Zn_2Cl_6]$ from $\chi_{ZnCl_2} = 0.50$, and $[C_2mim]_2\{Zn_4Cl_{10}\}$ from $\chi_{ZnCl_2} = 0.75$. The crystallographic details are shown in Table 7.

The crystal structure of $[C_2mim]_2[ZnCl_4]$ (which is isostructural with its cobalt(II) and nickel(II) analogues)[64] consists of $[C_2mim]^+$ cations and $[ZnCl_4]^{2-}$ anions. The $[ZnCl_4]^{2-}$ anions are surrounded by four imidazolium cations bound through strong directional C−H···Cl hydrogen bonds (see Figure 9a, with two cations eliminated for clarity).[65] All three ring protons of the imidazolium cations are involved in hydrogen bonding, with the H^2 proton showing the strongest hydrogen bond of 2.5720(7) Å and the H^4 and H^5 binding to two adjacent $[ZnCl_4]^{2-}$ anions, each at shorter distances of 2.7009(7) and 2.7558(7) Å and longer distances of 2.9206(7) and 2.9932(7) Å (Figure 9b), respectively.

Because each imidazolium cation is hydrogen-bonded (via both the ring protons and two *N*-methyl protons) to four adjacent $[ZnCl_4]^{2-}$ anions, this results for the ion packing in a complex three-dimensional C−H···Cl hydrogen-bond network. Because zinc atoms are located on a center of symmetry

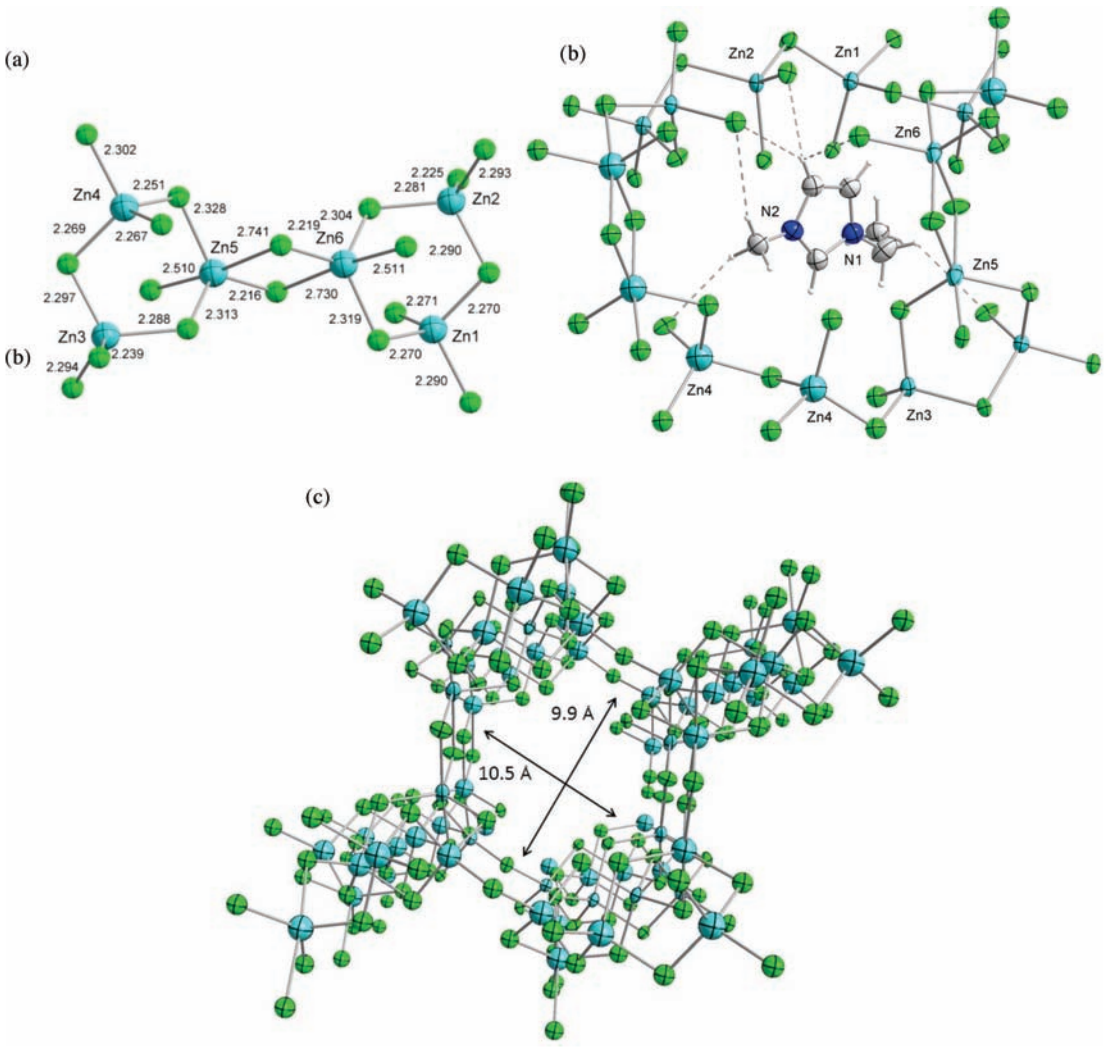

Figure 10. Crystal structure of $[C_2mim]_2\{Zn_4Cl_{10}\}$, obtained for $\chi_{ZnCl_2} = 0.75$: (a) cutout from the framework structure, showing the building units with corner-sharing tetrahedra and edge-sharing trigonal bipyramids; (b) framework structure with an anion in the cavity; (c) channel in the framework structure.

(space group $I4_1/a$), a regular tetrahedral coordination with Zn1−Cl and Zn2−Cl distances of 2.2736(7) and 2.2757(7) Å, respectively, is found.

The crystal structure of $[C_2mim]_2[Zn_2Cl_6]$ consists of $[C_2mim]^+$ cations and $[Zn_2Cl_6]^{2-}$ anions. The $[Zn_2Cl_6]^{2-}$ anions are surrounded by four imidazolium cations bound through strong directional C−H···Cl hydrogen bonds,[65] with distances ranging from 2.6783(5) to 2.9513(5) Å, as shown in Figure 9c (two cations eliminated for clarity). An inversion center is located at the center of the anion. The zinc atoms show a slightly distorted tetrahedral coordination, with $\bar{r}(\text{Zn−Cl}_{\text{bridging}})$ = 2.3486(6) and 2.3746(6) Å and $\bar{r}(\text{Zn−Cl}_{\text{terminal}})$ = 2.2021(6) and 2.2202(6) Å. Each imidazolium cation is hydrogen-bonded to two adjacent $[Zn_2Cl_6]^{2-}$ anions. $[C_2mim]_2[Zn_2Cl_6]$ exhibits a three-dimensional C−H···Cl hydrogen-bonded network.

The crystal structure of $[C_2mim]_2\{Zn_4Cl_{10}\}$ consists of an anionic three-dimensional chlorozincate framework with $[C_2mim]^+$ cations located in the cavities. The structure of $[C_2mim]_2\{Zn_4Cl_{10}\}$ contains six crystallographically independent zinc atoms in the asymmetric unit (Figure 10a). The anionic $\{Zn_4Cl_{10}\}^{2-}$ framework exhibits a centric arrangement leading to *pseudo*centrosymmetry in this noncentrosymmetric crystal structure (space group *C*2). Therefore, only three different zinc coordination environments can be distinguished. Zn1/Zn4 and Zn2/Zn3 adopt a slightly distorted tetrahedral coordination, with Zn−Cl distances ranging from 2.225(4) to 2.302(3) Å and Cl−Zn−Cl angles ranging from 101.3(1)° to 116.9(1)°. Zn5/Zn6 adopts an approximately trigonal-bipyramidal coordination, with three short equatorial Zn−Cl distances ranging from 2.216(4) to 2.329(3) Å and two longer axial bonds from 2.510(4) to 2.741(4) Å. The coordination for zinc shows an approximate trigonal bipyramid with *pseudo*-D_{3h} symmetry and with axial elongation. The axial Cl_{ax}−Zn−Cl_{ax} angles are 174.3(1)° and 174.8(1)°, respectively. The axial−equatorial Cl_{ax}−Zn−Cl_{eq} angles are from 85.8(1)° to 98.2(1)°.

The H^5 proton of the imidazolium ring forms very long contacts with three surrounding chloride atoms, with distances ranging from 2.925(3) to 2.952(3) Å (Figure 10b). Additionally, two *N*-methyl protons and one of the *N*-ethyl protons form contacts ranging from 2.795(3) to 2.969(3) Å.

The only report on a five-coordinate chlorozincate sturcture is that of Xie et al.,[66] claiming the existence of the anion

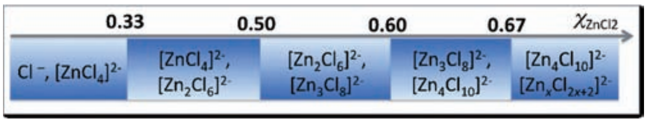

Figure 11. Suggested liquid-phase speciation of chlorozincate(II) ionic liquids, where $[Zn_xCl_{2x+2}]^{2-}$ ($x > 4$) are postulated polynuclear species.

$[ZnCl_5]^{3-}$ with a strangely distorted geometry. However, the crystal structure data, which purport to show a disordered anion, have been interpreted incorrectly and actually contain tetrachlorozincate anions, $[ZnCl_4]^{2-}$, with a positional disorder around a 2-fold rotational axis because the distances and angles would match well with this tetrahedral geometry. This explains the differences between the temperature factors in the reported refinement between "axial" and "equatorial" chloride atoms, in accordance with calculations by Gorinchoi et al.,[67] predicting the instability of a free $[ZnCl_5]^{3-}$ anion. Notably, all of the reported structures with a A_3ZnCl_5 (A = Cs, Rb, and NH_4) stoichiometry are actually tetrachlorozincates, $[ZnCl_4]^{2-}$, with an additional noncoordinating chloride anion.[68] To the best of our knowledge, the chlorozincate structure reported here, $[C_2mim]_2\{Zn_4Cl_{10}\}$, is therefore the first true example containing zinc in a five-coordinate chloride environment.

Martin and Greenwood[69] reported the crystal structure of $[H_2NEt_2]\{Cu^IZn^{II}{}_5Cl_{12}\}$, which forms a microporous framework. This rare structure has been called a halozeotype because it forms a class of nonoxide analogues of zeolite-like materials and adopts a sodalite structure with corner-sharing tetrahedral building blocks. The structure of $[C_2mim]_2\{Zn_4Cl_{10}\}$ adopts a different open framework because the building units are corner-sharing tetrahedra and edge-sharing trigonal bipyramids. To our knowledge, this is therefore a novel type of framework structure. The largest channels in the framework are formed along the *b* axis. The smallest ring that circumscribes the channel consists of 10 zinc atoms with the shortest Cl···Cl cross-channel distances of 6.65 and 7.34 Å and Zn···Zn distances across the channel of 9.9 and 10.5 Å (Figure 10c).

These chlorozincate(II) structures can be related to other known structures in the CCDC. Chlorozincate(II) salts ($\chi_{ZnCl_2} = 0.50$) with small cations, like potassium[70] or tetramethylammonium,[15b] contain polymeric anions. Shifting to bulkier cations, a search in the organic crystal structure database revealed that, among over 660 chlorozincate structures, a vast majority contained only $[ZnCl_4]^{2-}$,[71] sometimes with additional chloride ions. About 20 structures containing dimeric $[Zn_2Cl_6]^{2-}$ were found,[72] also coexisting with the tetrachlorozincate anion.[73] One other structure was discovered, containing the discrete tetranuclear $[Zn_4Cl_{10}]^{2-}$ anion with T_d (adamantane) symmetry.[74] Importantly, no structures were found containing singly charged chlorozincate(II) anions, including specifically $[ZnCl_3]^-$, $[Zn_2Cl_5]^-$, or $[Zn_3Cl_7]^-$.

■ CONCLUSIONS

The speciation of the $[C_8mim]Cl-ZnCl_2$ ionic liquid system has been resolved. Combining the data reported in this paper, determined on the liquid phase (Raman spectra, DSC, and Lewis acidity), with the critically analyzed published data, we propose that the anionic speciation involves chloride and a range of doubly charged chlorozincate(II) anions, as described in Figure 11. This is in stark contrast to the commonly accepted model, which contains only mononegative anions, and was based on an analogy with chloroaluminate(III) ionic liquids. Our conclusions are reinforced by a study by Abbott et al. (currently in press),[75] which detected the tetrachlorozincate(II) species in basic deep eutectics of zinc(II) chloride, cholinium chloride, and either ethylene glycol or urea.

The single-crystal X-ray diffraction study of the solid $[C_2mim]Cl-ZnCl_2$ system confirmed the existence of the $[ZnCl_4]^{2-}$ and $[Zn_2Cl_6]^{2-}$ anions in the solid phase, as found in the neat liquid. In contrast, the structure that crystallized from $\chi_{ZnCl_2} = 0.75$, $[C_2mim]_2\{Zn_4Cl_{10}\}$, revealed an open-framework structure with the first example of zinc in a trigonal-bipyramidal chloride coordination, which clearly cannot exist in a liquid phase.

The speciation presented here contradicts the results of a number of studies based on mass spectrometry (a gas-phase technique), which had been interpreted in terms of the presence of monocharged chlorozincate(II) species in the liquid phase. The ESI-MS experiments carried out in this work confirmed the presence of such monocharged anions in the ionized gas phase, but there was no evidence for their existence in the liquid phase. It was therefore concluded that the anionic speciation of this system is phase-dependent, and one should not assume that the species present in the liquid phase are the same as those in the solid or gaseous phases. More generally, this observation raises the question of the validity of all of the liquid-state speciation studies based on mass spectrometry and suggests that many previous studies, which relied on this technique, should be revisited.

■ ASSOCIATED CONTENT

Ⓢ Supporting Information. CIFs for the three presented crystal structures, ESI(−)-MS multiplets with assignments to the corresponding clusters, and DSC traces. This material is available free of charge via the Internet at http://pubs.acs.org.

■ AUTHOR INFORMATION

Corresponding Author

*E-mail: quill@qub.ac.uk.

■ ACKNOWLEDGMENT

The authors thank Dr. J. D. Holbrey (QUILL) for valuable comments and discussions and Prof. A. P. Abbott for supplying us with a manuscript of his paper in press prior to its publication. P.N. thanks the EPSRC for a RCUK fellowship. Moreover, the authors acknowledge QUILL and its Industrial Advisory Board, as well as the EPSRC (Portfolio Partnership Scheme, Grant EP/D029538/1), for support. The EPSRC UK National Crystallography Service is acknowledged for crystal data collection.

■ REFERENCES

(1) Wasserscheid, P.; Welton, T. *Ionic Liquids in Synthesis*, 2nd ed.; Wiley Interscience: Weinheim, Germany, 2007.

(2) Estager, J.; Oliferenko, A. A.; Seddon, K. R.; Swadźba-Kwaśny, M. *Dalton Trans.* **2010**, *39*, 11375.

(3) Wasserscheid, P.; Keim, W. *Angew. Chem., Int. Ed.* **2000**, *39*, 3773.

(4) (a) Hussey, C. L. *Adv. Molten Salt Chem.* **1983**, *5*, 185.(b) Tsuda, T.; Hussey, C. L. In *Modern Aspects of Electrochemistry*; White, R. I., Vayenas, C. G., Gamboa-Aldeco, M. E., Eds.; Springer: Dortrecht, The Netherlands, 2009; Vol. 45, p 63.

(5) Øye, H. A.; Jagatoyen, M.; Oksefjel, T.; Wilkes, J. S. *Mater. Sci. Forum* **1991**, *73*–*75*, 183.

(6) Welton, T. *Chem. Rev.* **1999**, *99*, 2071.

(7) Carpenter, M. K.; Verbrugge, M. W. *J. Mater. Res.* **1994**, *9*, 2584.

(8) Yang, J. Z.; Tian, P.; Xu, W. G.; Xu, B.; Liu, S. Z. *Thermochim. Acta* **2004**, *412*, 1.

(9) Apperley, D. C.; Hardacre, C.; Licence, P.; Murphy, R. W.; Plechkova, N. V.; Seddon, K. R.; Srinivasan, G.; Swadźba-Kwaśny, M.; Villar-Garcia, I. J. *Dalton Trans.* **2010**, *39*, 8679.

(10) Wicelinski, S. P.; Gale, R. J.; Wilkes, J. S. *J. Electrochem. Soc.* **1987**, *134*, 262.

(11) (a) Wicelinski, S. P.; Gale, R. J.; Wilkes, J. S. *Thermochim. Acta* **1988**, *126*, 255. (b) Wicelinski, S. P.; Gale, R. J.; Williams, S. D.; Mamantov, G. *Spectrochim. Acta, Part A* **1989**, *45*, 759. (c) Wicelinski, S. P.; Gale, R. J.; Pamidimukkala, K. M.; Lane, R. A. *Anal. Chem.* **1988**, *60*, 2228.

(12) Hardacre, C.; Murphy, R. W.; Seddon, K. R.; Srinivasan, G.; Swadźba-Kwaśny, M. *Aust. J. Chem.* **2010**, *63*, 845.

(13) Sitze, M. S.; Schreiter, E. R.; Patterson, E. V.; Freeman, R. G. *Inorg. Chem.* **2001**, *40*, 2298.

(14) Abbott, A. P.; Capper, G.; Davies, D. L.; Rasheed, R. *Inorg. Chem.* **2004**, *43*, 3447.

(15) For example, see: (a) Martin, J. D.; Dattelbaum, A. M.; Thornton, T. A.; Sullivan, R. M.; Yang, J.; Peachey, M. T. *Chem. Mater.* **1998**, *10*, 2699. (b) Choi, M.-H.; Kim, S.-H.; Chang, H.-Y.; Halasyamani, P. S.; Ok, K. M. *Inorg. Chem.* **2009**, *48*, 8376. (c) Pattacini, R.; Jie, S.; Braunstein, P. *Chem. Commun.* **2009**, 890. (d) Hu, G. Z.; Holt, E. M. *Acta Crystallogr., Sect. C* **1994**, *50*, 1212. (e) Halvorson, K. E.; Grigereit, T.; Willett, R. D. *Inorg. Chem.* **1987**, *26*, 1716. (f) Schaltin, S.; Nockemann, P.; Thijs, B.; Binnemans, K.; Fransaer, J. *Electrochem. Solid-State Lett.* **2007**, *10*, D104.

(16) Sun, H. J.; Harms, K.; Sundermeyer, J. *J. Am. Chem. Soc.* **2004**, *126*, 9550.

(17) (a) Taubert, A. *Angew. Chem., Int. Ed.* **2004**, *43*, 5380. (b) Taubert, A.; Steiner, P.; Mantion, A. *J. Phys. Chem. B* **2005**, *109*, 15542. (c) Taubert, A.; Palivan, C.; Casse, O.; Gozzo, F.; Schmitt, B. *J. Phys. Chem. C* **2007**, *111*, 4077.

(18) Abbott, A. P.; Capper, G.; Mckenzie, K. J.; Ryder, K. S. *J. Electroanal. Chem.* **2007**, *599*, 288.

(19) Calderon Morales, R.; Tambyrajah, V.; Jenkis, P. R.; Davies, D. L.; Abbott, A. P. *Chem. Commun.* **2004**, 158.

(20) Abbott, A. P.; Bell, T. J.; Handa, S.; Stoddart, B. *Green Chem.* **2005**, *7*, 705.

(21) Duan, Z.; Gu, Y.; Deng, Y. *Catal. Commun.* **2006**, *7*, 651.

(22) For example, see: (a) Neve, F.; Francescangeli, O.; Crispini, A. *Inorg. Chim. Acta* **2002**, *338*, 51. (b) Martin, J. D.; Keary, C. L.; Thornton, T. A.; Novotnak, M. P.; Knutson, J. W.; Folmer, J. C. W. *Nat. Mater.* **2006**, *5*, 271.

(23) Golubeva, E. N.; Kokorin, A. I.; Kochubei, D. I.; Pergushov, V. I.; Kriventsov, V. V. *Kinet. Catal.* **2002**, *43*, 408. *Kinet. Katal.* **2002**, *43*, 440.

(24) Abbott, A. P.; Capper, G.; Davies, D. L.; Munro, H. L.; Rasheed, R. K.; Tambyrajah, V. *Chem. Commun.* **2001**, 2010.

(25) (a) Lin, Y.; Sun, I. *Electrochim. Acta* **1999**, *44*, 2771. (b) Chen, P.; Lin, M.; Sun, I. *J. Electrochem. Soc.* **2000**, *147*, 3350. (c) Dupont, J.; Suarez, P. A. Z.; Umpierre, A. P.; de Souza, R. F. *Catal. Lett.* **2001**, *73*, 211.

(26) Koura, N.; Endo, T.; Idemoto, Y. *J. Non-Cryst. Solids* **1996**, *205*, 650.

(27) Lin, Y.-F.; Sun, I.-W. *J. Electrochem. Soc.* **1988**, *134*, 262.

(28) Liu, Y.; Wu, G.; Qi, M. *J. Cryst. Growth* **2005**, *281*, 616.

(29) Lecocq, V.; Graille, A.; Santini, C. C.; Baudouin, A.; Chauvin, Y.; Basset, J. M.; Arzel, L.; Bouchu, D.; Fenet, B. *New J. Chem.* **2005**, *29*, 700.

(30) Hsiu, S.-I.; Huang, J.-F.; Sun, I.-W.; Yuan, C.-H.; Shiea, J. *Electrochim. Acta* **2002**, 4367.

(31) Zou, Y.; Xu, H.; Wu, G.; Jiang, Z.; Chen, S.; Huang, Y.; Huang, W.; Wei, X. *J. Phys. Chem. B* **2009**, *113*, 2066.

(32) Alves, M. B.; Santos, V. O., Jr.; Soares, V. C. D.; Suarez, P. A. Z. *J. Raman Spectrosc.* **2008**, *39*, 1388.

(33) Alves, M. B.; Umpierre, A. P.; Santos, V. O., Jr.; Soares, V. C. D.; Dupont, J. M.; Rubim, J. C.; Suarez, P. A. Z. *Thermochim. Acta* **2010**, *502*, 20.

(34) Sheldrick, G. M. *Acta Crystallogr., Sect. A* **2008**, *64*, 112.

(35) Dolomanov, O. V.; Bourhis, L. J.; Gildea, R. J.; Howard, J. A. K.; Puschmann, H. *J. Appl. Crystallogr.* **2009**, *42*, 339.

(36) Gutmann, V. *The Donor–Acceptor Approach to Molecular Interactions*; Plenum Press: New York, 1978.

(37) Zhong, C.; Sasaki, T.; Jimbo-Kobayashi, A.; Fujiwara, E.; Kobayashi, A.; Tada, M.; Iwasawa, Y. *Bull. Chem. Soc. Jpn.* **2007**, *80*, 2365.

(38) For example, see: (a) Suter, R. W.; Knachel, H. C.; Petro, V. P.; Howatson, J. H.; Shore, S. G. *J. Am. Chem. Soc.* **1973**, *95*, 1474. (b) Dekock, R. L.; Gray, H. B. *Chemical Structure and Bonding*, 2nd ed.; University Science Books: Mill Valley, CA, 1989; p 87.

(39) Kebarle, P.; Tang, L. *Anal. Chem.* **1993**, *65*, 972A.

(40) Hussey, C. L. *Adv. Molten Salt Chem.* **1983**, *5*, 185.

(41) Fannin, A. A.; Floreani, D. A.; King, L. A.; Landers, J. S.; Piersma, B. J.; Stech, D. J.; Vaughn, R. L.; Wilkes, J. S.; Williams, J. L. *J. Phys. Chem.* **1984**, *88*, 2614.

(42) Stone, F. G. A., West, R., eds.; *Advances in Organometallic Chemistry*; Academic Press: London, 1970; Vol. 9, p 22.

(43) Hardacre, C. *Annu. Rev. Mater. Res.* **2005**, *35*, 29.

(44) Prince, R. H. In *Comprehensive Coordination Chemistry*; Wilkinson, G., Gillard, R. D., McCleverty, J. A., Eds.; Pergamon Press: Oxford, U.K., 1987; Vol. 5, p 981.

(45) (a) Strohalm, M.; Hassman, M.; Košata, B.; Kodíček, M. *Rapid Commun. Mass Spectrom.* **2008**, *22*, 905. (b) Strohalm, M.; Kavan, D.; Novak, P.; Volny, M.; Havlicek, V. *Anal. Chem.* **2010**, *82*, 4648.

(46) Kebarle, P. *J. Mass Spectrom.* **2000**, *35*, 804.

(47) Di Marco, V. B.; Bombi, G. G. *Mass Spectrom. Rev.* **2006**, *25*, 347.

(48) Di Marco, V. B.; Bombi, G. G.; Ranaldo, M.; Traldi, P. *Rapid Commun. Mass Spectrom.* **2007**, *21*, 3825.

(49) Di Marco, V. B.; Bombi, G. G.; Zambon, S.; Traldi, P. *J. Mass Spectrom.* **2009**, *44*, 120.

(50) Di Marco, V. B.; Raveane, L.; Dean, A.; Traldi, P. *Rapid Commun. Mass Spectrom.* **2010**, *24*, 868.

(51) Schroder, E.; Munster, H.; Budzikiewicz, H. *Org. Mass Spectrom.* **1986**, *21*, 707.

(52) Sunner, J.; Morales, A.; Kebarle, P. *Anal. Chem.* **1987**, *59*, 1378.

(53) Kosevich, M. V.; Shelkovsky, V. S.; Boryak, O. A.; Orlov, V. V. *Rapid Commun. Mass Spectrom.* **2003**, *17*, 1781.

(54) For example, see: (a) Jackson, G. P.; Duckworth, D. C. *Chem. Commun.* **2004**, 522. (b) Milman, B. L.; Alfassi, Z. B. *Eur. J. Mass Spectrom.* **2005**, *11*, 35.

(55) For example, see: Franzen, G.; Gilbert, B. P.; Pelzer, G.; DePauw, E. *Org. Mass Spectrom.* **1986**, *21*, 443.

(56) For example, see: Abdul-Sada, A. K.; Greenway, A. M.; Seddon, K. R.; Welton, T. *Org. Mass Spectrom.* **1993**, *28*, 759.

(57) Quicksall, C. O.; Spiro, T. G. *Inorg. Chem.* **1966**, *5*, 2232.

(58) Babushkina, O. B.; Volkov, S. V. *J. Mol. Liq.* **1999**, *83*, 131.

(59) Yannopoulos, S. N.; Kalampounias, A. G.; Chrissanthopoulos, A.; Papatheodorou, G. N. *J. Chem. Phys.* **2003**, *118*, 319.

(60) Ferraro, J. R. *Low Frequency Vibrations of Inorganic and Coordination Compounds*; Plenum Press, New York, 1971; p 173.

(61) McNaught, A. D., Wilkinson, A., Eds. *IUPAC: Compendium of Chemical Terminology (the "Gold Book")*, 2nd ed.; Blackwell Scientific Publications: Oxford, U.K., 1997. Online version: Nic, M.; Jirat, J.; Kosata, B.; updates by Jenkins, A. http://goldbook.iupac.org.

(62) (a) Zawodzinski, T. A., Jr.; Osteryoung, R. A. *Inorg. Chem.* **1989**, *28*, 1710. (b) Mantz, R. A.; Trulove, P. C.; Carlin, R. T.; Theim, T. L.; Osteryoung, R. A. *Inorg. Chem.* **1997**, *36*, 1227.

(63) Lipstajn, M.; Osteryoung, R. A. *Electrochem. Soc.* **1983**, *130*, 1968.

(64) Hitchcock, P. B.; Seddon, K. R.; Welton, T. *J. Chem. Soc., Dalton Trans.* **1993**, 2639.

(65) van den Berg, J. A.; Seddon, K. R. *Cryst. Growth Des.* **2003**, *3*, 643.

(66) Xie, Y. M.; Chen, W. T.; Wu, J. H. *J. Solid State Chem.* **2008**, *181*, 1853.

(67) Gorinchoi, N. N.; Bersuker, I. B.; Polinger, V. Z. *New J. Chem.* **1993**, *17*, 125.

(68) For example, see: Fejfarova, K.; Ouarsal, R.; El Bali, B.; Dusek, M.; Lachkar, M. *Acta Crystallogr., Sect. E* **2007**, *63*, i136.

(69) Martin, J. D.; Greenwood, K. B. *Angew. Chem., Int. Ed.* **1997**, *36*, 2072.

(70) Itoh, M.; Sakai, K.; Nakamura, T. *Inorg. Chem.* **1982**, *21*, 3552.

(71) For example, see: (a) Madariaga, G.; Zuniga, F. J.; Perez-Mato, J. M.; Tello, M. J. *Acta Crystallogr., Sect. B* **1987**, *43*, 356. (b) Pattacini, R.; Jie, S.; Braunstein, P. *Chem. Commun.* **2009**, 890.

(72) For example, see: (a) Pattacini, R.; Jie, S.; Braunstein, P. *Chem. Commun.* **2009**, 890. (b) Martin, J. D.; Dattelbaum, A. M.; Thornton, T. A.; Sullivan, R. M.; Yang, J.; Peachey, M. T. *Chem. Mater.* **1998**, *10*, 2699. (c) Weng, W.; Bartik, T.; Johnson, M. T.; Arif, A. M.; Gladysz, J. A. *Organometallics* **1995**, *14*, 889.

(73) Sun, W. Y.; Xie, J.; Okamura, T.; Huang, C. K.; Ueyama, N. *Chem. Commun.* **2000**, 1429.

(74) Bottomley, F.; Boyle, P. D.; Karslioglut, S.; Thompson, R. C. *Organometallics* **1993**, *12*, 4090.

(75) Abbott, A. P.; Barron, J. C.; Frisch, G.; Gurman, S.; Ryder, K. S.; Silva, A. F. *Phys. Chem. Chem. Phys.* **2011**accepted for publication.